Global deletome profile of Saccharomyces cerevisiae exposed to lithium

Nicolas Fierling, Patrick Billard, Pascale Bauda, Damien Blaudez

Global deletome profile of *Saccharomyces cerevisiae* exposed to lithium

Nicolas Fierling[1], Patrick Billard[1], Pascale Bauda[2], Damien Blaudez[1]

[1] Université de Lorraine, CNRS, LIEC, Vandœuvre-lès-Nancy, France,

[2] Université de Lorraine, CNRS, LIEC, Metz, France.

[#] Corresponding author:

Dr Damien Blaudez

UMR 7360 LIEC, Faculté des Sciences et Technologies

Université de Lorraine, BP70239

Vandoeuvre-lès-Nancy F-54506, France

Tel: +33-3-72-74-51-67

E-mail: damien.blaudez@univ-lorraine.fr

Abstract

The increasing use of lithium (Li) in new technologies raises the question of its impact on living microorganisms. In the present study, we aimed to identify putative Li targets and resistance mechanisms in the yeast model *Saccharomyces cerevisiae* using a deletomic approach based on the screening of a collection of 4,733 knockout mutants under Li exposure. This screening highlighted 60 mutants resistant to Li and 124 mutants sensitive to Li. Through functional enrichment analyses, transport systems and catabolite repression were identified as playing a central role in cell resistance to toxic concentrations of Li. In contrast, the AKT/protein kinase B family, signal transduction or cell communication were identified as potential toxic targets of Li. The majority of the mutants with a Li-sensitive phenotype were also sensitive to other alkali and alkaline-earth metals, whereas the Li-resistance phenotype was mostly resistant to Na but poorly resistant to other metals. A comparison with the results of deletomics studies carried out in the presence of other metals highlighted Li-specific phenotypes. Three genes (*NAM7*, *NMD2*, *UPF3*) of the nonsense-mediated decay pathway were specifically involved in resistance to Li. In contrast, mutants with the *NCA2*, *SPT20*, *GCN5*, *YOR376W*, *YPK3*, and *DCW1* genes deleted were specifically sensitive to Li. These genes encode various functions from putative mannosidase to constitution of the Spt-Ada-Gcn5 acetyltransferase complex. This work provides a better understanding of potential specific resistance mechanisms and cellular targets of Li in yeast.

Keywords: genome-wide screening, lithium-specific phenotypes, transport systems, signalling, yeast.

Graphical abstract

Yeast deletomics under lithium stress.

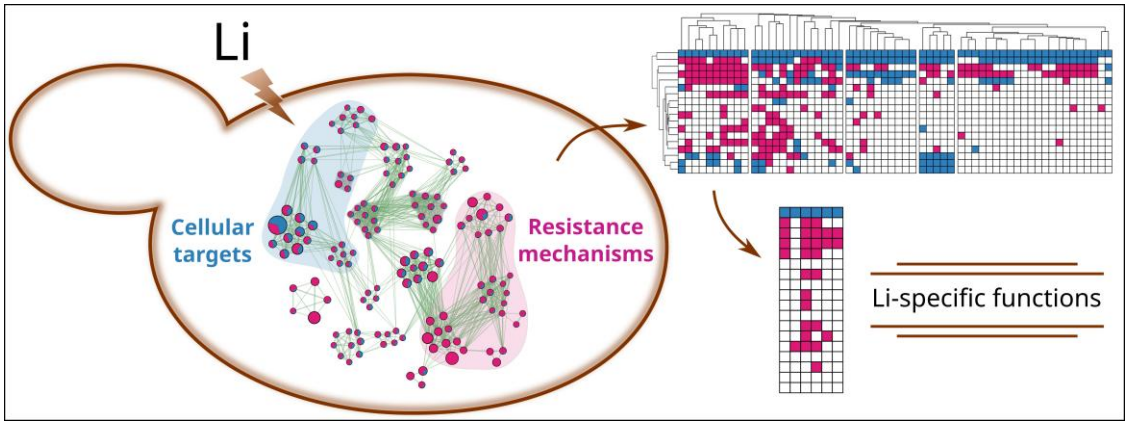

Introduction

Lithium (Li) has become an essential element in industry due to many of its physical and chemical properties (*e.g.*, low density, high specific heat capacity, high redox potential value) [1]. It is used in various fields, such as medicine (< 4%), ceramics and glass (14%), polymers (2%) and especially the manufacture of batteries (74%) [2]. The use of Li for batteries has almost doubled in 6 years [1] due to the growing demand for electric vehicles [2]. In addition, a forecast study estimated a 250% increase in Li demand by 2035 [3]. The exponential demand associated with a low recycling rate (expensive, energy consuming and polluting methods for the most part) [4,5] leads to significant Li dissemination in the environment [6,7]. Currently, Li is present in relatively low concentrations in soil and sea water (~ 40 ppm and ~ 150 µg/L, respectively) [6,8,9], but high concentrations can be found, especially near extraction areas, from 200 to 1000 ppm [6].

Li is not an essential element for living organisms, which may explain the absence of Li-specific transport systems. However, Li is able to cross biological membranes through Na or K transporters. In *Saccharomyces cerevisiae*, ENA (Exitus NAtru, a subfamily of P-type ATPase) transporters allow the export of Li^+ as well as Na^+ [10]. Nha1p, a Na^+/H^+ antiporter, is also involved in the efflux of Li^+ [11]. Conversely, Marquina et al., (2012) highlighted that the K^+-transporter Trk1,2p can import Li^+ and consequently trigger intracellular toxic effects on yeast cells. Li has been shown to inhibit Hal2p and the RNase MRP, impacting the maturation of RNA [13], delaying sporulation [14], increasing protein aggregation and reducing cell volume [15]. Furthermore, Li can inhibit Pgm2p, a phosphoglucomutase, by competing with its cofactor Mg^{2+} [16]. In conclusion, literature data related to Li cellular targets and resistance mechanisms remain fragmentary and deserve more genome-wide investigation.

The yeast model *S. cerevisiae* has been extensively used to study the tolerance mechanisms and cellular targets of various toxic compounds, mainly by screening collections of nonessential mutants [17–24]. In a previous work, genome-wide screening in the presence of LiCl identified 114 Li-sensitive mutants, highlighting the involvement of meiosis, sporulation and vacuoles in the tolerance of yeast to Li [25]. However, since high concentrations of LiCl were used for the screening of Li-responsive mutants, it could be hypothesized that high concentrations of the counteranion (Cl^-) could trigger false positives. In the same study, six Li-resistant mutants were reported; however, this limited number of

mutants prevented a thorough analysis of Li toxicity targets. Therefore, the first objective of our study was to revisit the search for Li-responsive genes in yeast by performing a series of screening steps including the use of two Li salts to eliminate false positives. A deep functional analysis was then performed to elucidate the functions involved in Li sensitivity or resistance. The second objective was to study the specificity of these functions between alkali metals and alkaline earth metals. To this aim, the Li-specific functions were investigated by exposing the retained mutants to four alkali and alkaline earth metals (Na, Mg, K and Ca). By combining these results, we provide evidence of specific phenotypes to Li and those shared among alkali metals and alkaline-earth metals.

Materials and Methods

Yeast strains and medium

A collection of KO deletion mutants for each of the 4,733 nonessential genes of *Saccharomyces cerevisiae* was used (Euroscarf; haploid BY4741 background; MATa *his*3Δ1 *leu*2Δ0 *met*15Δ0 *ura*3Δ0). All experiments were performed with YPD medium at pH 6.5 (per litre: 10 g yeast extract, 20 g peptone, 20 g glucose, 15 g agar if required).

Genome-wide screening with Li

The library screening consisted of a three-step approach to identify and validate Li-sensitive and Li-resistant mutants. The primary mutant screening consisted of a qualitative assessment of their growth response on Li-agar plates. For this purpose, the individual deleted mutants were first grown in 200 µL of YPD in 96-well microplates at 28°C with agitation (160 rpm) from stationary phase cultures. The mutants were subsequently replicated on YPD agar plates supplemented or not supplemented with lithium chloride (LiCl, Sigma Aldrich, Saint-Quentin-Fallavier, France) by using a Thermo Scientific Nunc Replication System. Four replicas were performed per mutant. Two ranges of Li concentrations were first tested on a sub-set of the library: 600, 650, and 700 mM and 850, 900, 950, and 1000 mM to find the best conditions to identify the sensitive and resistant mutants, respectively. We found that the 600 mM condition was the best option to identify sensitive mutants. Similarly, 900 and 1000 mM Li were chosen to select resistant mutants. In conclusion, the 4,733 mutants were tested in the presence of these three Li concentrations as well as on Li-free YPD. The plates were photographed and analysed after 5 days of growth at 28°C. Li-sensitive and Li-resistant mutants were identified by visual inspection as decreases or increases in their colony size,

respectively, compared to that of the WT on Li-amended medium. Li-free plates were also used as growth controls.

A secondary screening was performed with the previously identified sensitive and resistant mutants to confirm the phenotypes obtained. The mutants were grown overnight in 200 µL of YPD in a 96-well microplate at 28°C with agitation (160 rpm). Tenfold serial dilutions were carried out, and 5 µL drops of each dilution were spotted on plates with two ranges of LiCl: 300 to 600 mM and 650 to 1000 mM (by 50 mM increment steps in both cases) to validate the phenotype of sensitive and resistant mutants, respectively. After 5 days of growth, the mutants were considered sensitive when they exhibited no growth for at least one order of dilution relative to the WT. Conversely, the mutants were considered resistant when they showed additional growth for at least one order of dilution compared to the WT.

The tertiary screening consisted of a validation screening in liquid cultures. The mutants validated from the secondary screening were grown overnight in 5 mL of YPD and then inoculated (OD_{600nm} = 0.05) in the presence of a range of LiCl concentrations in 96-well microplates: 0 to 400 mM (by 50 mM increments) or 0 to 600 mM (by 100 mM increments) to confirm the sensitivity or resistance of the mutants, respectively. The microplates were incubated for 24 hours before measuring OD_{600nm} with a spectrophotometer (Xenius SAFAS, Monaco). As an additional validation step, a quaternary screening was performed. It consisted of the same strategy as in the tertiary screening but with another Li salt (Li_2SO_4. H_2O, Sigma Aldrich). To this end, a concentration range of 50, 100 to 500 mM Li (by 100 mM increments) was used. The data were normalized to those obtained at 0 mM Li, and a growth percentage in relation to the WT was calculated.

Finally, for both the tertiary and quaternary screenings, the mutants were classified according to their percentage of sensitivity or resistance compared to the WT. Mutants exhibiting less than 50% growth at 50 mM Li were classified as high-sensitivity (HS) mutants. Between 50% and 90% growth at 50 mM Li, the mutants were classified as medium-sensitivity (MS) mutants. The sensitive mutants exhibiting growth above 90% at both 100 mM and 150 mM Li were grouped in the low-sensitivity (LS) category. Mutants exhibiting growth above 150% at 100 mM Li were classified as high-resistance (HR) mutants. Mutants exhibiting growth between 110% and 150% at 100 mM Li were classified as medium-resistance (MR) mutants. Finally, the resistant mutants displaying growth below 110% at 200 mM were grouped in the low-resistance (LR) category.

Cross-comparison of Li-responsive mutants with other metals

To investigate the potential Li-specific phenotypes of the mutants, liquid growth assays were performed in the presence of toxic concentrations of other alkali or alkaline-earth metals: $MgCl_2.6H_2O$ (0.8 to 1.8 M); KCl (1 to 2 M); NaCl (0.8 to 1.7 M); $CaCl_2.2H_2O$ (100 to 500 mM). For these four compounds, 100 mM increments were tested.

The mutants identified in the present study were also compared with those reported from other screenings carried out on yeast KO mutant libraries on Al [23,26], As [21,22,27–29], Cd [28–31], Co [17], Cr [28,32], Cu [17,24,28,33], Fe [17,24,33], Mn [17,24,34], Ni [17,30,35], Zn [17,24,28,36], Y [19], Yb and La [18]. When similar independent studies on the same stressor were performed, the corresponding lists of mutants were combined. Clustering and heatmaps were generated using the R package pheatmap.

EC50 determination

For the Li-specific responsive mutants obtained from the quaternary screening, their EC_{50} values for Li were determined. The mutants and WT were inoculated (OD_{600nm} = 0.05) with a range (0 to 500 mM by 50 mM increments) of LiCl in 96-well microplates. Biological triplicates were performed. The microplates were incubated for 24 hours at 28°C and 160 rpm. The OD_{600nm} was recorded, and the EC_{50} values were calculated using R software with the ec50estimator package.

Gene function and functional enrichment analysis

Gene descriptions of the sensitive and resistant mutants were retrieved from the Saccharomyces Genome Database (SGD). Biological process (p value < 0.01) and cellular compartment (p value < 0.05) were analysed using MIPS and FunSpec [37], respectively. The functions involved in the mechanisms of sensitivity and resistance to Li were determined with functional enrichment. This analysis was carried out on the mutants from the quaternary screening. The enrichment was calculated using Metascape software (*p value* < 0.01) [38] and visualized with Cytoscape v3.9.1 software [39] with default settings (maximum of 10 functions visualized per cluster).

Determination of cellular Li concentrations

The mutants and WT were grown in liquid YPD medium (28°C, 160 rpm). Cultures were inoculated at an OD_{600nm} of 0.1 and incubated until reaching an OD_{600nm} of 1. The cells were then exposed for 1 hour to 100 mM LiCl, a concentration corresponding to the EC_{10} of the WT. The cells (from 100 mL cultures) were harvested by centrifugation (4000 rpm, 1 min, 4 °C) and washed three times with ice-cold MES (20 mM)-EDTA (10 mM) buffer (pH 6) and then three times with ice-cold ultrapure water. The pellets were dried at 60 °C for 24 h. Five

and three independent biological replicates were prepared for the WT and the mutants, respectively. Concentrations of Li, macroelements and microelements were determined using inductively coupled plasma–mass spectrometry (Thermo iCap-TQ-ICP–MS, Thermo Fisher Scientific, Courtaboeuf, France). Cell pellets (approximately 60 mg DW) were mineralized with 1.75 mL HNO_3 and 0.5 mL H_2O_2 in DigiPREP tubes placed in a block digestion system (DigiPREP, SCP Sciences, Courtaboeuf, France). The samples were gradually heated to 100 °C over a 180 min period. The volume was completed to 12.5 mL with ultrapure water followed by filtration to 1 µm. The results are expressed as micrograms of element per gram of cell DW. The validity of the analytical method was verified by a standard reference material (oriental basma tobacco leaves, INCT-OBTL-5).

Statistical analysis

The statistical tests were performed using R software (version 4.1.2). Two-tailed Student's *t test* to compare the different conditions to WT was performed. EC_{50} values are the means ± standard deviations of biological triplicates. Values of Li concentrations in cells are the means ± standard errors of three or five independent replicates for the mutants and the WT, respectively.

Results and Discussion

Identification of a large set of Li-responsive genes

The screening of the 4,733 mutants was performed by four successive steps under Li exposure to identify sensitive and resistant mutants (Supplemental Figure S1). The primary screening identified a total of 327 sensitive mutants and 240 resistant mutants (Figure 1). Therefore, a secondary screening was carried out with the drop test method (Supplemental Figure S1) to refine the results and confirmed 155 (47%) sensitive and 96 (40%) resistant mutants (Figure 1). To further eliminate remaining putative false positives possibly arising from unequal amounts of cell inoculum, a tertiary screening consisting of liquid cultures exposed to Li was performed by individually normalizing the initial OD of all liquid cultures (Supplemental Figure S1). The mutants were then classified into six categories according to their level of sensitivity and resistance, from high sensitivity (HS) to high resistance (HR) (Tables 1&2). On the one hand, 59 low sensitivity (LS), 50 moderate sensitivity (MS), 31 HS and 15 false-positive mutants were identified. On the other hand, 18 low-resistance (LR), 35 medium-resistance (MR), 28 HR and 15 false-positive mutants were identified. Finally, to exclude sensitive/resistant phenotypes stemming from the accompanying chloride anion of the LiCl

206 salt used, the same test was repeated in a quaternary screening with Li_2SO_4. This comparison
207 confirmed a large majority (89%) of the Li-sensitive mutants (n=124) (Figure 1, Table 1).
208 Mutants that were lost (sensitive to LiCl but not to Li_2SO_4) belonged essentially to the LS
209 category. Indeed, 76, 96 and 100% of LS, MS and HS mutants from the tertiary screening in
210 the presence of LiCl were also sensitive to Li_2SO_4 (Supplemental Figure S2A). Similarly, but
211 to a lesser extent, 70% of the LiCl-resistant mutants were also resistant to Li_2SO_4 (n=60)
212 (Figure 1, Table 2). In more detail, 56, 74 and 86% of LR, MR and HR mutants were resistant
213 to both Li salts, respectively (Supplemental Figure S2B). The high conservation rate of the
214 HS and HR mutants after this quaternary screening suggests functions that are critical to the
215 cell response in the presence of Li.

216 Variable results can be encountered when screening experiments of the same metal are
217 performed in yeast. For example, for Cu screenings, Jo et al., (2008) found 89 sensitive
218 mutants, compared to three for Wang et al., (2007) and 170 for Bleackley et al., (2011).
219 Similarly, 18 [24], 89 [36] and 130 [17] sensitive mutants were retrieved for Zn genome-wide
220 screenings, and 67 [34] versus 141 [17] sensitive mutants were found in two Mn deletomics
221 screenings. The differences that were observed could originate from variations in the yeast
222 mutant collection, medium composition, culture conditions, screening method and/or the
223 arbitrary threshold used to define a sensitivity/resistance phenotype. In the case of Li, a
224 similar screening to the one described here was performed with LiCl and reported 114 Li-
225 sensitive and 6 Li-resistant mutants [25]. Seventy-three sensitive and all (6) resistant mutants
226 were found in common with our primary screening. Since the same medium (YPD) was used
227 in both studies, the difference could be explained by the fact that a slightly different yeast
228 mutant collection was used in this study (BY4743 homozygous diploid mutants versus
229 BY4741 haploid mutants in our study). However, the differences we observed are more likely
230 the result of using a different screening method. Zhao et al., (2010) screened their collection
231 on agar plates with a replicator, followed by colony streaking to confirm sensitive and
232 resistant mutants. However, this screening used a single concentration of Li, and there was no
233 mention about cell quantity normalization when the confirmation screening on agar plates was
234 performed. Moreover, high concentrations (several hundreds of mM) of LiCl were used to
235 achieve toxicity in yeast cells. As an adverse consequence, the Li false positives that arose in
236 both studies could be due to the toxic effects of the counteranion (chloride). This problem was
237 circumvented in the present study by using another Li salt (Li_2SO_4). Finally, 40 (35%)
238 sensitive and 4 (7%) resistant mutants from Zhao et al., (2010) were found in our quaternary

screening. Among these mutants, 24, 22 and 45% of LS, MS and HS mutants were identified in the present study, respectively (Supplemental Figure S3). Another yeast mutant screening was performed with $LiPF_6$, a Li-ion battery electrolyte [20], but identified only four and five mutants in common with the study of Zhao et al., (2010) and the present study, respectively (Supplemental Figure S3). This high discrepancy is very likely due to the extreme cytotoxicity of $LiPF_6$, where a concentration of 3-5 mM was sufficient to inhibit yeast growth in YPD medium. The authors concluded that the $LiPF_6$-mediated toxicity was not due to Li but to the $LiPF_6$ compound itself. In conclusion, and compared to these two previous reports, the screening performed here allowed the identification of a consequent batch (80) of new Li-sensitive mutants (Supplemental Figure S3). These mutants belong in similar proportions to the LS, MS and HS categories, notably highlighting new proteins playing an important role in Li resistance in yeast. Moreover, this conclusion is all the more true for Li-resistant mutants (60 mutants; Table 2), for which 10 times more mutants were reported and confirmed here with two lithium salts.

Conserved functions involved in yeast resistance to alkali and alkaline-earth metals

The study of the sensitive mutants allowed us to highlight the functions involved in yeast resistance under Li stress. These functions were revealed by a functional enrichment analysis (Figure 2). Whereas most of the clusters grouped functions that gathered both sensitive and resistant mutants, the endosomal transport, cytosolic transport, endocytosis, and cellular response to abiotic stimulus clusters gathered nearly exclusively sensitive mutants (Figure 2A). However, among the different clusters, some corresponded to functions for which the majority of sensitive mutants was found and for which the enrichment ratio (k/f) was the highest (Supplemental Table S1). This was the case for endocytosis (*p* value = 1.70E-03) endosomal transport (*p* value = 9.14E-09), cytosolic transport (*p* value = 6.48E-05), vacuole organization (*p* value = 2.95E-05), and vacuolar transport clusters (*p* value = 4.81E-08) composed of 91, 89, 89, 88 and 82% sensitive mutants, of which 50, 36, 50, 40 and 34% were HS, respectively (Figures 2A & 2B, Supplemental Table S1).

The majority of the 124 mutants were found to show a phenotype sensitive to alkali metals and alkaline earth metals (Figure 3). A similarity of 94, 84, 85 and 72% with the Li dataset was indeed found for Mg, K, Na and Ca, respectively (Supplemental Table S2). More globally, 75 of the 124 mutants (60%) exhibited sensitivity to the five alkali/alkaline-earth metals (Supplemental Figure S4A). Sixteen other mutants (13%) also shared a sensitive

phenotype but were not sensitive to Ca. The functional enrichment analysis revealed that three of the clusters described above were also retrieved for the other alkali and alkaline-earth elements (Figure 2B). The clusters endosomal transport (*p* value = 9.14E-09), cytosolic transport (*p* value = 9.37E-05), endocytosis (*p* value = 1.70E-03) (Supplemental Table S1) were indeed represented under at least three other metals. Negative regulation of cellular process, regulation of cellular component organization, and viral life cycle – HIV-1 clusters were identified in the presence of five metals. Conversely, the AKT family and cell communication clusters were evidenced under Mg and K, and Na and K, respectively. Three other functional clusters (regulation of nucleobase metabolism, regulation of biological quality and chromatin organization with a *p value* of 7.46E-08, 2.37E-05 and 3.18E-04, respectively) (Supplemental Table S1) were less represented but were found for the three alkali metals and Mg. Similarly, the clusters macromolecule catabolic process, regulation of transport, and signal transduction were only identified under Na or Mg stress.

Interestingly, four other clusters were Li-specific and included vacuolar transport (*p value* = 4.81E-08), vacuole organization (*p* value = 2.95E-05), cellular response to abiotic stimulus (*p* value = 2.36E-04), and transcription process (*p value* = 2.74E-04) (Figure 2B). These clusters were composed of 34, 40, 12 and 42% HS mutants, respectively (Figure 2B). The high representation of HS mutants suggests that the genes belonging to these clusters could play a key role in the Li-specific resistance of yeast.

The high concentrations of Li salts used in the media could trigger osmotic stress in yeast cells. To investigate the extent to which osmotic stress favoured the retrieval of sensitive mutants, we compared our sensitive mutant dataset with that obtained from a study focusing on osmotic stress mediated by high Na [40] (Supplemental Figure S5). Out of the 124 Li-sensitive mutants, only nine mutants were found in common with those identified in the previous study. Therefore, the high majority of the sensitive mutants found in the present study are very likely Li-responsive and not osmotic stress-responsive.

As described above, several functional clusters involved in metal transport were retrieved. Notably, the endosomal transport cluster was found for the five metals tested but was threefold larger in diameter for Li (15%) than for the other metals (6 to 9%). Similarly, the vacuolar transport cluster was Li-specific and the cluster regulation of transport was only common between Li and Na. Combined with the high number of HS mutants found in the transport functions (>30%), our data confirm the central role of transport systems in Li resistance**.** Li entry into yeast cells can be nonspecifically handled by K^+- [41] or Na^+- [11]

transporters. As reported by Zhao *et al*. (2010), we found that the *TRK1* mutant was HS to Li (Table 1), Moreover, the *HAL5* mutant was also sensitive to Li in our study. Hal5p, the halotolerance protein kinase C, is a regulator of the K transporter Trk1p [11] and was shown to be a high-copy suppressor of numerous Li-sensitive mutations of genes involved in sporulation, meiosis and biosynthesis of ergosterol [25], a major compound of membranes in yeast. Conversely, Ena5p and Nha1p allow the efflux of both Na and Li out of the cells [10,11]. The *ENA* mutants are not included in the EUROSCARF library and were therefore not tested. However, several *ENA* genes (*ENA1*, *ENA2*, *ENA5*) are present in the BY4741 strain and have a very similar function (salt tolerance, and possibly Li tolerance). Nha1p is a Na^+/H^+ antiport whose activity varies according to the external pH. At pH 7, the quantity of lithium that was effluxed was 4 and 6 times lower than those at pH 5.5 and 3.5, respectively [42]. Our screening was performed at pH 6.5, therefore in this condition, the role of Nha1p in Li efflux could be minor compared to that played by the ENA proteins, explaining why this mutant was not found as sensitive. Li and Na ions have a very similar ionic radius [43], most likely explaining this nonspecificity. Li accumulation in the vacuole also occurs [44], but the transport system has not yet been identified. Under Li stress, yeast could partly internalize Li in vacuoles, thus limiting its toxicity. In line with this hypothesis, 14 mutants involved in vacuolar protein sorting (VPS) [45,46] were retrieved in the present study.

Finally, a comparative analysis of sensitive mutants was derived from an *in silico* analysis using the experimental data described above for alkali metals and alkaline earth metals as well as from the literature data reporting similar yeast mutant screenings with transition metals and lanthanides (Figure 3, Supplemental Table S3). The sensitive phenotype was poorly conserved when considering other elements (Figure 3). Three clusters (#4, #6, #8) out of the eight that were identified were characterized by rare mutants exhibiting a phenotype sensitive to transition metals and lanthanides. In these clusters, functions involved in nucleotide binding, RNA degradation or modification by phosphorylation could be listed. However, a high similarity of the response was found for As (41%) and Cd (52%). This was the case for a majority of mutants retrieved within clusters #1, #2, #3, #5, #7 that showed a predominance of the phenotype sensitive to As and Cd (Figure 3) and gathering vacuolar/lysosomal transport (*VAM7*, *VPS25*, *VPS1*, *VPS51*, *SNF7*, *PEP3*, *VPS34*, *VPS33*, *ARP5*, *VPS75*, *VPS27*, *PEP12*, *SNF8*, *VPS16*, *VPS28*, *BRO1*, *VMA11*, *VPS4*), regulation of C-compound and carbohydrate metabolism (*CCR4*, *PTC1*, *PBS2*, *VPS25*, *SNF7*, *HOG1*, *PFK2*, *SNF8*, *TAF14*) or actin cytoskeleton (*SLA1*, *SAC6*, *MNN10*, *VPS52*, *PBS2*, *VRP1*, *END3*). Yeast tolerance to As and Cd was reported to be managed through vacuolar internalization

[47,48]. Furthermore, Perkins and Gadd (1993) reported that Li was mainly compartmentalized in the yeast vacuole. Taken together, these data reinforce the idea that vacuolar transport is an important mechanism in the resistance of *S. cerevisiae* to Li. Another cluster (#2) showed a particular pattern. The 12 mutants from this cluster exhibited a sensitive phenotype to most of the metals, except Al, for which a very low number of mutants were retrieved from the screening [23,26]. This cluster was composed of 50% HS mutants, and vacuolar/lysosomal transport was the main function identified. This cluster therefore groups mutants for which the deleted genes likely play a common role in mediating resistance to a large set of metals, including Li, possibly by sequestering metals into vacuoles. However, taking all the results together, the present data indicate that the sensitive phenotype of the mutants is highly conserved for alkali metals and alkaline earth metals but poorly conserved with transition metals and lanthanides.

Proteins of the NMD pathway are specifically involved in Li resistance

Considering the whole set of Li-sensitive mutants and all metals tested, we investigated mutants specifically sensitive to Li. Only three mutants specifically sensitive to Li were identified: *NAM7* (alias *UPF1*), *NMD2* (alias *UPF2*) and *UPF3*. The mutants for the two first genes were categorized as LS, whereas the third one was classified as MS from the quaternary screening. The encoded UPF proteins are part of the NMD (nonsense-mediated mRNA decay) pathway that recognizes and degrades mRNAs containing premature termination codons [49–52].

To quantify the tolerance of the WT and the UPF mutants, EC50 values were determined from liquid cultures and a range of Li concentrations. The three mutants harboured significantly lower EC50 values compared to that of the WT, approximately 140 mM Li for the *UPF* mutants versus 175 mM for the WT (Figure 4A), confirming the Li-sensitive phenotype of these mutants. Yeast sensitivity to metals is often related to higher metal accumulation by cells. Therefore, we investigated the Li content of the mutants in the presence of a nonlethal concentration (EC10) of Li. There was no significant difference in Li accumulation between *UPF3* and WT cells (Figure 4B). Conversely, the *NMD2* and *NAM7* mutants significantly accumulated 1.9 and 1.7 times more Li than the WT strain. This higher accumulation of Li very likely induced a concomitant higher toxicity for cells. We hypothesize that this Li overaccumulation phenotype could be due either to a higher Li entry into cells or to a lower efflux out of cells. However, a Li efflux experiment was performed

and revealed that Li efflux was similar for the three mutants and the WT (data not shown), refuting the second hypothesis. Therefore, Li entry into cells is likely to be more important in NMD mutants, explaining the higher toxicity that was observed.

The NMD pathway could modulate metal ion homeostasis and detoxification. Indeed, Zhang and Kebaara (2022) reported that the transport of Mg, Zn, Cu, Cd and Fe was regulated by the NMD pathway, either by acting directly on the transporter or indirectly through a regulator. Mutating one of the three UPF genes increased yeast tolerance to Cu by regulating COX mRNAs in the mitochondria [54]. Conversely, if lactate, a nonfermentable carbon source, was used, the single *UPF* mutants had a growth response similar to that of the WT under Cu stress [55]. In the case of Li, how the NMD pathway interacts with Li homeostasis remains an open question. However, considering the opposite phenotype of the *UPF* mutants under Cu and Li stresses, the mRNA targets are likely different under Cu and Li exposure. Since the NMD pathway regulates hundreds of genes in yeast [56], detailed investigations are needed to decipher which UPF gene(s) are involved and identify their targets under Li stress. Some genes may be specifically regulated by only one of the three UPF proteins. Notably, it was reported that NAM7 affects the translation of the phosphoglucomutase PGM2 by interacting with its 5' UTR, explaining the high sensitivity to Li of the *PGM2* mutant in a medium containing galactose as the sole source of C [57]. Nevertheless, the majority of the mRNAs that are targets of NMD are regulated by the three UPF proteins [56]. As the three UPF mutants were all sensitive to Li in the present study, their targets under Li stress could be the same. However, this point deserves further attention, especially since *UPF* mutants were the only Li-specific mutants. Moreover, as functions of the NMD pathway are conserved in eukaryotic organisms [58], this pathway could also participate in Li resistance in other eukaryotes by eliminating abnormal mRNAs produced under Li stress.

Li-resistant mutants are mostly resistant to Na but show dissimilar behaviour toward other metals

The study of resistant mutants allowed us to identify the functions involved in yeast sensitivity under Li stress. A comparative mutant clustering analysis showed that the patterns were globally conserved under Li and Na (Figure 5, Supplemental Table S4). Indeed, 41 mutants out of 60 were both Li- and Na-resistant (Supplemental Figure S4B, Supplemental Table S2). Conversely, among the Li-resistant mutants, only 16 and 13 mutants were resistant to Ca and K, respectively. Moreover, only two resistant mutants were found for Mg. One

cluster (#1) out of five grouped 10 Li-resistant mutants that were all sensitive to all other alkali metals and alkaline earth metals. Interestingly, four out of the 10 mutants corresponded to deleted genes encoding transcription regulators (e.g., Gzf3p, Spt20p, Gcn5p and Ngg1p). Other clusters (#2-5) grouped mutants that were mostly resistant to both Li and Na but rarely to other metals.

Unlike sensitive mutants, as revealed by the functional enrichment analysis (Figure 2A & 2B), no cluster was uniquely involved in the resistance phenotype (Figure 2A). This could be due to a twofold lower number of resistant mutants obtained from the quaternary screening (Figure 1). However, among the clusters where the proportion of resistant mutants was the highest, chromatin organization (*p value* = 3.18E-04), signal transduction (*p value* = 5.23E-04), AKT family (*p value* = 2.08E-05), cell communication (*p value* = 3.05E-05) or transcription process (*p value* = 9.97E-06) were found and composed of 38, 37, 36, 35 and 34% resistant mutants, of which 25, 17, 50, 44 and 40% were HR, respectively (Figure 2B, Supplemental Table S1). The main cluster gathering the functions involved in yeast sensitivity was the AKT family cluster and was also retrieved, but to a lesser extent, from the functional enrichment analysis in the presence of Mg and K (36% for Li against 21% and 24% for Mg and K, respectively) (Figure 2B). Similarly, the four other clusters described above also had a proportion of resistant mutants that was higher under Li stress than under other alkali and alkaline-earth metals (Figure 2B). A functional analysis of the genes found in these five clusters indicated that they were mainly related to phosphorylation/dephosphorylation and acetylation/deacetylation activities (*p* value = 8.28E-12). Protein synthesis initiation is a target of salt toxicity [11]. Indeed, mutation of the protein kinase Gcn2p improves salt tolerance [59]. This kinase regulates the initiation of protein synthesis by phosphorylating the initiation factor eIF2 [60]. Gcn2p is overactivated during Na stress, which is deleterious for cell growth. Given the high similarity of responses between Na and Li found in the present study, we could hypothesize a similar impact of Li on protein translation mediated by phosphorylation/dephosphorylation (Npr1p, Sky1p, Ypk3p, Ypk1p) and acetylation/deacetylation (Spt20p, Gcn5p, Ngg1p, Spt8p, Pdb1p) activities of proteins found within these clusters, which would consequently affect yeast survival under Li stress. Altogether, our data highlight that the potential toxicity targets are similar for Li and Na but dissimilar for other alkali, alkaline earth, and transition metals.

A small set of genes are specifically involved in Li cytotoxicity

The screening allowed the identification of six mutants specifically resistant to Li (Figure 5). These mutants were *YOR376W* (MR), *DCW1* (LR), *NCA2* (HR), *YPK3* (MR), *GCN5* (LR), and *SPT20* (LR). The Li tolerance level of the WT and the six resistant mutants was further examined by determining the EC50 values. With EC50 varying between 189 mM and 315 mM for the mutants against 175 mM Li for WT, all the mutants had a higher EC50 than the WT, although for GCN5, the difference was not significant (Figure 6A). These results therefore confirmed the Li-resistance phenotype of these mutants.

Among the six Li-specific resistant mutants, *SPT20*, *GCN5* and *YPK3* were grouped in the peptidyl-amino acid modification cluster (Figure 2A, Supplemental Table S1). Spt20p and Gcn5p are part of the SAGA (Spt-Ada-Gcn5 acetyltransferase) complex [61], which regulates approximately 10% of the genes in *S. cerevisiae* [62]. It is a multifunctional complex involved in histone acetylation and deubiquitination [63,64] or in mRNA export [65]. Ypk3p is an AGC kinase (protein kinase A/protein kinase G/protein kinase C family) essential to the TORC1 pathway [66]. TORC1 denotes Target of Rapamycin Complex 1, one of the two complexes of the TOR pathway [67]. Genetic interactions between the SAGA complex and the TORC1 pathway have been demonstrated in *Schizosaccharomyces pombe* [68]. Interestingly, the SAGA complex was shown to control the expression of key genes needed for Cd tolerance in *S. pombe* [69]. The *GCN5* and *SPT20* KO mutants of *S. pombe* were among the most Cd-sensitive mutants. Similarly, in *S. cerevisiae*, these mutants were also reported as Cd-sensitive [31] (Figure 5). The components and functions of the SAGA complex are highly conserved between many species [70,71], which explains why the SAGA pathway likely plays a role in Cd resistance in both yeast species. However, in the present study, the opposite phenotype for Li was found for the *GCN5* and *SPT20* mutants (resistant mutants). We can therefore hypothesize that Gcn5p and Spt20p might regulate key genes other than those involved in the Cd response. This hypothesis could be extended to other alkali metals and alkaline earth metals since they also induced a sensitive phenotype for the *GCN5* and *SPT20* mutants (Figure 5). The SAGA complex is mainly considered an activator complex, but it can also inhibit some genes through Gcn5p, for instance [72]. In conclusion, our data suggest that the SAGA complex could (i) be involved in the activation of gene(s) responsible for Li sensitivity and/or (ii) repress gene(s) promoting Li resistance in yeast. We further investigated whether the Li resistance phenotype of these mutants could result from reduced Li accumulation in cells. The ICP–MS results obtained for Li accumulation in these three mutants were variable (Figure 6B). Indeed, the *YPK3* and *GCN5* mutants accumulated

1.7 and 1.2 times more Li than the WT, respectively, although it was not significant for *GCN5*. Conversely, *SPT20* accumulated 0.6 times less Li than the WT. These results demonstrate a different accumulation capacity for these Li-specific resistant mutants. Since Li accumulation was not reduced in *GNC5* and *YPK3* mutant cells, their Li-resistant phenotype is likely independent of Li accumulation and can be better explained if Gcn5p and Ypk3p are targets of Li.

The second group of Li-specific resistant mutants contained DCW1 and NCA2, which belong to the macromolecule catabolic process cluster, and YOR376W, a gene encoding a protein of unknown function (Figure 2A, Supplemental Table S1). DCW1 encodes a putative mannosidase that is essential for cell wall biogenesis. A mutation of DCW1 causes cell wall malformations [73]. NCA2 regulates the expression of the F0-F1 ATP synthase subunits [74]. In a genome-wide screening, the three mutants were found to affect vacuole membrane fragmentation under NaCl stress [75]. We hypothesized that a similar phenotype occurs for these mutants under Li stress. Induction of fragmentation would produce several small vacuoles, therefore diminishing the volume for storing Li and contributing to enhanced cytotoxicity. However, the three mutants harboured the opposite phenotype of resistance to Li, which is in disagreement with the given hypothesis. Moreover, the three mutants had a higher cellular Li content compared to the WT, although the data were only significant for the *YOR376W* mutant (Figure 6B). Altogether, our data suggest the existence of other, yet unknown, mechanisms. As described above for Gcn5p and Ypk3p, the resistant phenotypes of *DCW1*, *NCA2* and *YOR376W* were not accompanied by a reduction in Li content in cells and therefore can be better explained if these proteins are targets of Li.

Conclusion

An in-depth study of the results of Li screenings of a collection of KO mutants identified potential cellular targets and mechanisms of resistance to Li in yeast. Transport systems are involved in resistance to Li and other alkali/alkaline earth metals. The NMD pathway is a resistance mechanism specific to Li, a pathway generally involved in sensitivity to other metals. In contrast, the AKT family, signal transduction, chromatin organization, transcription process or cell communication are the main functions involved in Li sensitivity, with the SAGA complex as a Li-specific target. The majority of putative cellular targets are shared between Na and Li. Proteomic or transcriptomic studies should be designed to investigate these data further, notably to reveal the details of the roles played by the NMD pathway and

the SAGA complex under Li. In conclusion, the present data obtained on this eukaryotic model species suggest new perspectives to better understand the environmental impact of Li, a major emerging metallic contaminant, on living organisms.

Author contributions

Conceptualization: NF, PBa, PBi and DB, data analysis: NF, writing and editing the manuscript: NF, PBa, PBi and DB. Project management and financial support: PBa, DB. All the authors have read and approved the final manuscript.

Funding

This work was supported by the French National Research Agency through the National Program “Investissements d’Avenir” with the reference ANR-10-LABX-21-01/LABEX RESSOURCES 21.

Acknowledgements

We thank the pôle de compétences en chimie analytique, ANATELo (LIEC) for ICP–MS analyses. This work is included in the scientific program of the GISFI research consortium (Groupement d'Intérêt Scientifique sur les Friches Industrielles).

Conflict of interest

The authors declare no conflict of interest.

Data availability

All the data described is available in the online Supplemental material.

References

1. Swain B. Recovery and recycling of lithium: A review. *Sep Purif Technol* 2017;**172**:388–403.

2. United States Geological Survey Report of Mineral Commodities, 2022. U.S. Geological Survey, Mineral Commodity Summaries, January 2020.

3. Garside M. Statista, Chemicals & Ressources, Minin, Metals & Minerals. Projection of lithium demand worldwide from 2020 to 2035. 2023.

4. Bae H, Kim Y. Technologies of lithium recycling from waste lithium ion batteries: a review. *Mater Adv* 2021;**2**:3234–50.

5. Duan X, Zhu W, Ruan Z, Xie M, Chen J, Ren X. Recycling of lithium batteries—A review. *Energies* 2022;**15**:1611.

6. Bolan N, Hoang SA, Tanveer M, Wang L, Bolan S, Sooriyakumar P, Robinson B, Wijesekara H, Wijesooriya M, Keerthanan S, Vithanage M, Markert B, Fränzle S, Wünschmann S, Sarkar B, Vinu A, Kirkham MB, Siddique KHM, Rinklebe J. From mine to mind and mobiles – Lithium contamination and its risk management. *Environ Pollut* 2021;**290**:118067.

7. Mrozik W, Ali Rajaeifar M, Heidrich O, Christensen P. Environmental impacts, pollution sources and pathways of spent lithium-ion batteries. *Energy Environ Sci* 2021;**14**:6099–121.

8. Aral H, Vecchio-Sadus A. Lithium: environmental pollution and health effects. Elsevier, 2011, 499–508.

9. Aral H, Vecchio-Sadus A. Toxicity of lithium to humans and the environment--a literature review. *Ecotoxicol Environ Saf* 2008;**70**:349–56.

10. Prior C, Potier S, Souciet JL, Sychrova H. Characterization of the NHA1 gene encoding a Na+/H+-antiporter of the yeast Saccharomyces cerevisiae. *FEBS Lett* 1996;**387**:89–93.

11. Jakobsson E, Argüello-Miranda O, Chiu S-W, Fazal Z, Kruczek J, Nunez-Corrales S, Pandit S, Pritchet L. Towards a unified understanding of lithium action in basic biology and its significance for applied biology. *J Membr Biol* 2017;**250**:587–604.

12. Marquina M, González A, Barreto L, Gelis S, Muñoz I, Ruiz A, Álvarez MC, Ramos J, Ariño J. Modulation of yeast alkaline cation tolerance by Ypi1 requires calcineurin. *Genetics* 2012;**190**:1355–64.

13. Dichtl B, Stevens A, Tollervey D. Lithium toxicity in yeast is due to the inhibition of RNA processing enzymes. *EMBO J* 1997;**16**:7184–95.

14. Asensio J, Ruiz-Argüeso T, Rodríguez-Navarro A. Sensitivity of yeasts to lithium. *Antonie Van Leeuwenhoek* 1976;**42**:1–8.

15. Reith P, Braam S, Welkenhuysen N, Lecinski S, Shepherd J, MacDonald C, Leake MC, Hohmann S, Shashkova S, Cvijovic M. The effect of lithium on the budding yeast Saccharomyces cerevisiae upon stress adaptation. *Microorganisms* 2022;**10**:590.

16. Csutora P, Strassz A, Boldizsár F, Németh P, Sipos K, Aiello DP, Bedwell DM, Miseta A. Inhibition of phosphoglucomutase activity by lithium alters cellular calcium homeostasis and signaling in Saccharomyces cerevisiae. *Am J Physiol Cell Physiol* 2005;**289**:C58-67.

17. Bleackley MR, Young BP, Loewen CJR, MacGillivray RTA. High density array screening to identify the genetic requirements for transition metal tolerance in Saccharomyces cerevisiae. *Metallomics* 2011;**3**:195–205.

18. Grosjean N, Le Jean M, Chalot M, Mora-Montes HM, Armengaud J, Gross EM, Blaudez D. Genome-wide mutant screening in yeast reveals that the cell wall is a first shield to discriminate light from heavy lanthanides. *Front Microbiol* 2022;**13**:881535.

19. Grosjean N, Gross EM, Le Jean M, Blaudez D. Global deletome profile of Saccharomyces cerevisiae exposed to the technology-critical element yttrium. *Front Microbiol* 2018;**9**.

20. Jin X, Zhang J, An T, Zhao H, Fu W, Li D, Liu S, Cao X, Liu B. A Genome-wide screen in Saccharomyces cerevisiae reveals a critical role for oxidative phosphorylation in cellular tolerance to lithium hexafluorophosphate. *Cells* 2021;**10**:888.

21. Johnson AJ, Veljanoski F, O'Doherty PJ, Zaman MS, Petersingham G, Bailey TD, Münch G, Kersaitis C, Wu MJ. Molecular insight into arsenic toxicity via the genome-wide deletion mutant screening of Saccharomyces cerevisiae. *Metallomics* 2016;**8**:228–35.

22. Thorsen M, Di Y, Tängemo C, Morillas M, Ahmadpour D, Van der Does C, Wagner A, Johansson E, Boman J, Posas F, Wysocki R, Tamás MJ. The MAPK Hog1p modulates Fps1p-dependent arsenite uptake and tolerance in yeast. *Mol Biol Cell* 2006;**17**:4400–10.

23. Tun NM, O'Doherty PJ, Chen Z-H, Wu X-Y, Bailey TD, Kersaitis C, Wu MJ. Identification of aluminium transport-related genes via genome-wide phenotypic screening of Saccharomyces cerevisiae. *Metallomics* 2014;**6**:1558–64.

24. Wang J, Wang X, Fang Y, Zhou B. Genome-wide screening of yeast metal homeostasis genes involved in mitochondrial functions. *Mol Genet Genomics* 2007;**277**:673–83.

25. Zhao J, Lin W, Ma X, Lu Q, Ma X, Bian G, Jiang L. The protein kinase Hal5p is the high-copy suppressor of lithium-sensitive mutations of genes involved in the sporulation and meiosis as well as the ergosterol biosynthesis in Saccharomyces cerevisiae. *Genomics* 2010;**95**:290–8.

26. Kakimoto M, Kobayashi A, Fukuda R, Ono Y, Ohta A, Yoshimura E. Genome-wide screening of aluminum tolerance in Saccharomyces cerevisiae. *Biometals Int J Role Met Ions Biol Biochem Med* 2005;**18**:467–74.

27. Haugen AC, Kelley R, Collins JB, Tucker CJ, Deng C, Afshari CA, Brown JM, Ideker T, Van Houten B. Integrating phenotypic and expression profiles to map arsenic-response networks. *Genome Biol* 2004;**5**:R95.

28. Jin YH, Dunlap PE, McBride SJ, Al-Refai H, Bushel PR, Freedman JH. Global Transcriptome and deletome profiles of yeast exposed to transition metals. *PLOS Genet* 2008;**4**:e1000053.

29. Thorsen M, Perrone GG, Kristiansson E, Traini M, Ye T, Dawes IW, Nerman O, Tamás MJ. Genetic basis of arsenite and cadmium tolerance in Saccharomyces cerevisiae. *BMC Genomics* 2009;**10**:105.

30. Ruotolo R, Marchini G, Ottonello S. Membrane transporters and protein traffic networks differentially affecting metal tolerance: a genomic phenotyping study in yeast. *Genome Biol* 2008;**9**:R67.

31. Serero A, Lopes J, Nicolas A, Boiteux S. Yeast genes involved in cadmium tolerance: Identification of DNA replication as a target of cadmium toxicity. *DNA Repair* 2008;**7**:1262–75.

32. Johnson AJ, Veljanoski F, O'Doherty PJ, Zaman MS, Petersingham G, Bailey TD, Münch G, Kersaitis C, Wu MJ. Revelation of molecular basis for chromium toxicity by phenotypes of Saccharomyces cerevisiae gene deletion mutants. *Metallomics* 2016;**8**:542–50.

33. Jo WJ, Loguinov A, Chang M, Wintz H, Nislow C, Arkin AP, Giaever G, Vulpe CD. Identification of genes involved in the toxic response of Saccharomyces cerevisiae against iron and copper overload by parallel analysis of deletion mutants. *Toxicol Sci Off J Soc Toxicol* 2008;**101**:140–51.

34. Chesi A, Kilaru A, Fang X, Cooper AA, Gitler AD. The role of the Parkinson's disease gene PARK9 in essential cellular pathways and the manganese homeostasis network in yeast. *PloS One* 2012;**7**:e34178.

35. Arita A, Zhou X, Ellen TP, Liu X, Bai J, Rooney JP, Kurtz A, Klein CB, Dai W, Begley TJ, Costa M. A genome-wide deletion mutant screen identifies pathways affected by nickel sulfate in Saccharomyces cerevisiae. *BMC Genomics* 2009;**10**:524.

36. Pagani MA, Casamayor A, Serrano R, Atrian S, Ariño J. Disruption of iron homeostasis in Saccharomyces cerevisiae by high zinc levels: a genome-wide study. *Mol Microbiol* 2007;**65**:521–37.

37. Robinson MD, Grigull J, Mohammad N, Hughes TR. FunSpec: a web-based cluster interpreter for yeast. *BMC Bioinformatics* 2002;**3**:35.

38. Zhou Y, Zhou B, Pache L, Chang M, Khodabakhshi AH, Tanaseichuk O, Benner C, Chanda SK. Metascape provides a biologist-oriented resource for the analysis of systems-level datasets. *Nat Commun* 2019;**10**:1523.

39. Shannon P, Markiel A, Ozier O, Baliga NS, Wang JT, Ramage D, Amin N, Schwikowski B, Ideker T. Cytoscape: a software environment for integrated models of biomolecular interaction networks. *Genome Res* 2003;**13**:2498–504.

40. Auesukaree C, Damnernsawad A, Kruatrachue M, Pokethitiyook P, Boonchird C, Kaneko Y, Harashima S. Genome-wide identification of genes involved in tolerance to various environmental stresses inSaccharomyces cerevisiae. *J Appl Genet* 2009;**50**:301–10.

41. Marquina Rodríguez M, González A, Barreto L, Gelis S, Munoz Munoz I, Ruiz A, Alvarez M, Ramos J, Ariño J. Modulation of yeast alkaline cation tolerance by Ypi1 requires calcineurin. *Genetics* 2012;**190**:1355–64.

42. Kinclová O, Potier S, Sychrová H. Difference in substrate specificity divides the yeast alkali-metal-cation/H(+) antiporters into two subfamilies. *Microbiol Read Engl* 2002;**148**:1225–32.

43. Shannon RD. Revised effective ionic radii and systematic studies of interatomic distances in halides and chalcogenides. *Acta Crystallogr Sect A* 1976;**32**:751.

44. Perkins J, Gadd GM. Accumulation and intracellular compartmentation of lithium ions in Saccharomyces cerevisiae. *FEMS Microbiol Lett* 1993;**107**:255–60.

45. Bonangelino CJ, Chavez EM, Bonifacino JS. Genomic screen for vacuolar protein sorting genes in Saccharomyces cerevisiae. *Mol Biol Cell* 2002;**13**:2486–501.

46. Robinson JS, Klionsky DJ, Banta LM, Emr SD. Protein sorting in Saccharomyces cerevisiae: isolation of mutants defective in the delivery and processing of multiple vacuolar hydrolases. *Mol Cell Biol* 1988;**8**:4936–48.

47. Ghosh M, Shen J, Rosen BP. Pathways of As(III) detoxification in Saccharomyces cerevisiae. *Proc Natl Acad Sci* 1999;**96**:5001–6.

48. Li Z-S, Lu Y-P, Zhen R-G, Szczypka M, Thiele DJ, Rea PA. A new pathway for vacuolar cadmium sequestration in Saccharomyces cerevisiae: YCF1-catalyzed transport of bis(glutathionato)cadmium. *Proc Natl Acad Sci U S A* 1997;**94**:42–7.

49. Cui Y, Hagan KW, Zhang S, Peltz SW. Identification and characterization of genes that are required for the accelerated degradation of mRNAs containing a premature translational termination codon. *Genes Dev* 1995;**9**:423–36.

50. He F, Jacobson A. Identification of a novel component of the nonsense-mediated mRNA decay pathway by use of an interacting protein screen. *Genes Dev* 1995;**9**:437–54.

51. Lee BS, Culbertson MR. Identification of an additional gene required for eukaryotic nonsense mRNA turnover. *Proc Natl Acad Sci U S A* 1995;**92**:10354–8.

52. Mitchell P, Tollervey D. An NMD pathway in yeast involving accelerated deadenylation and exosome-mediated 3'→5' degradation. *Mol Cell* 2003;**11**:1405–13.

53. Zhang X, Kebaara BW. Nonsense-mediated mRNA decay and metal ion homeostasis and detoxification in Saccharomyces cerevisiae. *BioMetals* 2022, DOI: 10.1007/s10534-022-00450-0.

54. Deliz-Aguirre R, Atkin AL, Kebaara BW. Copper tolerance of Saccharomyces cerevisiae nonsense-mediated mRNA decay mutants. *Curr Genet* 2011;**57**:421–30.

55. Murtha K, Hwang M, Peccarelli MC, Scott TD, Kebaara BW. The nonsense-mediated mRNA decay (NMD) pathway differentially regulates COX17, COX19 and COX23 mRNAs. *Curr Genet* 2019;**65**:507–21.

56. Celik A, Baker R, He F, Jacobson A. High-resolution profiling of NMD targets in yeast reveals translational fidelity as a basis for substrate selection. *RNA N Y N* 2017;**23**:735–48.

57. Hajikarimlou M, Hunt K, Kirby G, Takallou S, Jagadeesan S, Omidi K, Hooshyar M, Burnside D, Moteshareie H, Babu M, Smith M, Holcik M, Samanfar B, Golshani A. Lithium chloride sensitivity in yeast and regulation of translation. *Int J Mol Sci* 2020;**21**:5730.

58. Causier B, Li Z, De Smet R, Lloyd JPB, Van de Peer Y, Davies B. Conservation of nonsense-mediated mRNA decay complex components throughout eukaryotic evolution. *Sci Rep* 2017;**7**:16692.

59. Goossens A, Dever TE, Pascual-Ahuir A, Serrano R. The protein kinase Gcn2p mediates sodium toxicity in yeast. *J Biol Chem* 2001;**276**:30753–60.

60. Serrano R, Gaxiola R, Ríos G, Forment J, Vicente O, Ros R. Salt stress proteins identified by a functional approach in yeast. *Monatshefte Für Chem Chem Mon* 2003;**134**:1445–64.

61. Sterner DE, Grant PA, Roberts SM, Duggan LJ, Belotserkovskaya R, Pacella LA, Winston F, Workman JL, Berger SL. Functional organization of the yeast SAGA complex: distinct components involved in structural integrity, nucleosome acetylation, and TATA-binding protein interaction. *Mol Cell Biol* 1999;**19**:86–98.

62. Lee TI, Causton HC, Holstege FCP, Shen W-C, Hannett N, Jennings EG, Winston F, Green MR, Young RA. Redundant roles for the TFIID and SAGA complexes in global transcription. *Nature* 2000;**405**:701–4.

688 63. Daniel JA, Torok MS, Sun Z-W, Schieltz D, Allis CD, Yates JR, Grant PA. Deubiquitination of histone
689 H2B by a yeast acetyltransferase complex regulates transcription. *J Biol Chem* 2004;**279**:1867–71.

690 64. Grant PA, Duggan L, Côté J, Roberts SM, Brownell JE, Candau R, Ohba R, Owen-Hughes T, Allis CD,
691 Winston F, Berger SL, Workman JL. Yeast Gcn5 functions in two multisubunit complexes to acetylate
692 nucleosomal histones: characterization of an Ada complex and the SAGA (Spt/Ada) complex. *Genes*
693 *Dev* 1997;**11**:1640–50.

694 65. Rodríguez-Navarro S, Fischer T, Luo M-J, Antúnez O, Brettschneider S, Lechner J, Pérez-Ortín JE,
695 Reed R, Hurt E. Sus1, a functional component of the SAGA histone acetylase complex and the nuclear
696 pore-associated mRNA export machinery. *Cell* 2004;**116**:75–86.

697 66. González A, Shimobayashi M, Eisenberg T, Merle DA, Pendl T, Hall MN, Moustafa T. TORC1
698 promotes phosphorylation of ribosomal protein S6 via the AGC kinase Ypk3 in Saccharomyces
699 cerevisiae. *PLOS ONE* 2015;**10**:e0120250.

700 67. Guertin DA, Sabatini DM. Defining the role of mTOR in cancer. *Cancer Cell* 2007;**12**:9–22.

701 68. Laboucarié T, Detilleux D, Rodriguez-Mias RA, Faux C, Romeo Y, Franz-Wachtel M, Krug K, Maček
702 B, Villén J, Petersen J, Helmlinger D. TORC1 and TORC2 converge to regulate the SAGA co-activator in
703 response to nutrient availability. *EMBO Rep* 2017;**18**:2197–218.

704 69. Guo L, Ganguly A, Sun L, Suo F, Du L-L, Russell P. Global fitness profiling identifies arsenic and
705 cadmium tolerance mechanisms in fission yeast. *G3 Bethesda Md* 2016;**6**:3317–33.

706 70. Koutelou E, Hirsch CL, Dent SYR. Multiple faces of the SAGA complex. *Curr Opin Cell Biol*
707 2010;**22**:374–82.

708 71. Spedale G, Timmers HTM, Pijnappel WWMP. ATAC-king the complexity of SAGA during evolution.
709 *Genes Dev* 2012;**26**:527–41.

710 72. Ricci AR, Genereaux J, Brandl CJ. Components of the SAGA histone acetyltransferase complex are
711 required for repressed transcription of ARG1 in rich medium. *Mol Cell Biol* 2002;**22**:4033–42.

712 73. Kitagaki H, Wu H, Shimoi H, Ito K. Two homologous genes, DCW1 (YKL046c) and DFG5, are
713 essential for cell growth and encode glycosylphosphatidylinositol (GPI)-anchored membrane proteins
714 required for cell wall biogenesis in Saccharomyces cerevisiae. *Mol Microbiol* 2002;**46**:1011–22.

715 74. Camougrand N, Pélissier P, Velours G, Guérin M. NCA2, a second nuclear gene required for the
716 control of mitochondrial synthesis of subunits 6 and 8 of ATP synthase in Saccharomyces cerevisiae. *J*
717 *Mol Biol* 1995;**247**:588–96.

718 75. Michaillat L, Mayer A. Identification of genes affecting vacuole membrane fragmentation in
719 Saccharomyces cerevisiae. *PloS One* 2013;**8**:e54160.

720

721

Table 1: List of the 124 lithium-sensitive mutants identified from the quaternary screening.

The mutants were classified according to their level of sensitivity compared to the WT after exposure to a range of Li concentrations. Mutants inhibited by more than 50% at 50 mM Li were classified as highly sensitive. Mutants that had residual growth between 50% and 90% at 50 mM Li were classified as medium sensitive. Low-sensitivity mutants were those for which growth was below 90% at 100 mM and 150 mM Li.

Systematic name	Standard name	Systematic name	Standard name	Systematic name	Standard name	Systematic name	Standard name
High sensitive mutants (31/124)							
YCR008W	*SAT4*	YFR040W	*SAP155*	YKR001C	*VPS1*	YLR396C	*VPS33*
YDR069C	*DOA4*	YGL038C	*OCH1*	YKR020W	*VPS51*	YML008C	*ERG6*
YDR195W	*REF2*	YGL246C	*RAI1*	YLR025W	*SNF7*	YNL294C	*RIM21*
YDR207C	*UME6*	YGR056W	*RSC1*	YLR048W	*RPS0B*	YPL002C	*SNF8*
YDR245W	*MNN10*	YGR285C	*ZUO1*	YLR148W	*PEP3*	YPL045W	*VPS16*
YDR484W	*VPS52*	YHR141C	*RPL42B*	YLR192C	*HCR1*	YPL129W	*TAF14*
YDR532C	*KRE28*	YJL129C	*TRK1*	YLR226W	*BUR2*	YPL271W	*ATP15*
YER083C	*GET2*	YJR043C	*POL32*	YLR240W	*VPS34*		
Medium sensitive mutants (48/124)							
YBL006C	*LDB7*	YDR364C	*CDC40*	YLR056W	*ERG3*	YNL170W	-
YBL007C	*SLA1*	YEL050C	*RML2*	YLR113W	*HOG1*	YNL171C	-
YBL025W	*RRN10*	YGL012W	*ERG4*	YLR235C	-	YNL298W	*CLA4*
YBR082C	*UBC4*	YGL045W	*RIM8*	YLR262C	*YPT6*	YOR030W	*DFG16*
YBR200W	*BEM1*	YGL173C	*XRN1*	YLR322W	*VPS65*	YOR080W	*DIA2*
YCR094W	*CDC50*	YGR072W	*UPF3*	YLR330W	*CHS5*	YPL065W	*VPS28*
YDL006W	*PTC1*	YHR205W	*SCH9*	YMR031W-A	-	YPL084W	*BRO1*
YDL213C	*NOP6*	YJL006C	*CTK2*	YMR075W	*RCO1*	YPL157W	*TGS1*
YDR049W	*VMS1*	YJL075C	*APQ13*	YMR205C	*PFK2*	YPL234C	*VMA11*
YDR137W	*RGP1*	YJL165C	*HAL5*	YNL016W	*PUB1*	YPR045C	*THP3*
YDR138W	*HPR1*	YJR102C	*VPS25*	YNL059C	*ARP5*	YPR163C	*TIF3*
YDR293C	*SSD1*	YKL158W	*APE2*	YNL084C	*END3*	YPR173C	*VPS4*
Low sensitive mutants (45/124)							
YAL021C	*CCR4*	YDR389W	*SAC7*	YKL190W	*CNB1*	YNR006W	*VPS27*
YAR020C	*PAU7*	YFL013C	*IES1*	YKR035C	*OPI8*	YOR006C	*TSR3*
YBL024W	*NCL1*	YGL003C	*CDH1*	YKR072C	*SIS2*	YOR036W	*PEP12*
YBR036C	*CSG2*	YGL019W	*CKB1*	YKR073C	-	YOR141C	*ARP8*
YBR231C	*SWC5*	YGL046W	-	YLR039C	*RIC1*	YPL194W	*DDC1*
YBR246W	*RRT2*	YGL212W	*VAM7*	YLR234W	*TOP3*	YPR023C	*EAF3*
YDL001W	*RMD1*	YGR122W	-	YLR337C	*VRP1*	YPR135W	*CTF4*
YDL020C	*RPN4*	YHL027W	*RIM101*	YML057W	*CMP2*	YPR160W	*GPH1*
YDR072C	*IPT1*	YHR077C	*NMD2*	YMR080C	*NAM7*	YPR194C	*OPT2*
YDR127W	*ARO1*	YHR200W	*RPN10*	YNL064C	*YDJ1*		
YDR129C	*SAC6*	YIL076W	*SEC28*	YNL246W	*VPS75*		
YDR136C	*VPS61*	YJL128C	*PBS2*	YNL307C	*MCK1*		

Table 2: List of the 60 lithium-resistant mutants identified from the quaternary screening.

The mutants were classified according their level of resistance compared to the WT after exposure to a range of Li concentrations. Mutants harbouring a growth above 150% at 100 mM Li were classified as high resistance. Mutants exhibiting between 110% and 150% growth at 100 mM Li were classified as medium resistance. Low-resistance mutants had growth above 110% at 200 mM Li.

Systematic name	Standard name	Systematic name	Standard name	Systematic name	Standard name	Systematic name	Standard name
High resistant mutants (24/60)							
YBR085c-A	-	YER167W	*BCK2*	YJR078W	*BNA2*	YNL323W	*LEM3*
YBR121C	*GRS1*	YGL066W	*SGF73*	YKL126W	*YPK1*	YOR241W	*MET7*
YDL197C	*ASF2*	YGL095C	*VPS45*	YLR244C	*MAP1*	YOR375C	*GDH1*
YDR043C	*NRG1*	YGL168W	*HUR1*	YMR216C	*SKY1*	YPL062W	-
YDR199W	-	YIL130W	*ASG1*	YNL164C	*IBD2*	YPL137C	*GIP3*
YEL045C	-	YJL190C	*RPS22A*	YNL229C	*URE2*	YPR155C	*NCA2*
Medium resistant mutants (26/60)							
YAL049C	*AIM2*	YDR176W	*NGG1*	YLR391W	-	YOL114C	*PTH4*
YBR028C	*YPK3*	YDR297W	*SUR2*	YLR455W	*PDP3*	YOR220W	*RCN2*
YBR044C	*TCM62*	YJL024C	*APS3*	YML006C	*GIS4*	YOR376W	-
YCL001w-B	-	YKR055W	*RHO4*	YML016C	*PPZ1*	YPL061W	*ALD6*
YDL081C	*RPP1A*	YLR055C	*SPT8*	YMR116C	*ASC1*	YPL138C	*SPP1*
YDL133C-A	*RPL41B*	YLR374C	-	YMR269W	*TMA23*		
YDR112W	*IRC2*	YLR375W	*STP3*	YNL183C	*NPR1*		
Low resistant mutants (10/60)							
YBR221C	*PDB1*	YGR252W	*GCN5*	YKL046C	*DCW1*	YNR052C	*POP2*
YDR200C	*VPS64*	YJL028W	*YJL028W*	YMR172W	*HOT1*	YOL148C	*SPT20*
YEL046C	*GLY1*	YJL110C	*GZF3*				

740 **Table 3: MIPS subcellular compartments involved in Li stress.** k is the number of mutants
741 found from the quaternary screening. f is the total number of genes in a given function. NS:
742 not significant; ER: Endoplasmic reticulum.

		All mutants		Sensitive mutants		Resistant mutants	
Subcellular compartment	**f**	***p* value**	**k**	***p* value**	**k**	***p* value**	**k**
Endosome	57	2.17E-05	9	8.88E-06	8	NS	-
Cytoskeleton	107	2.65E-03	9	1.56E-04	9	NS	-
ER	537	6.29E-03	25	2.02E-03	20	NS	-
Golgi	125	7.40E-03	9	5.01E-04	9	NS	-
Cytoplasm	2879	1.63E-02	94	NS	-	NS	-
Nucleus	1976	2.56E-02	67	NS	-	1.45E-02	26
Vacuole	224	4.48E-02	11	8.71E-03	10	NS	-
Vacuolar membrane	98	NS	-	9.66E-03	6	NS	-
Actin cytoskeleton	54	NS	-	1.77E-02	4	NS	-
Golgi membrane	95	NS	-	3.17E-02	5	NS	-
ER membrane	131	NS	-	3.51E-02	6	NS	-
Nuclear envelope	167	NS	-	3.59E-02	7	NS	-

743

744

Figure legends

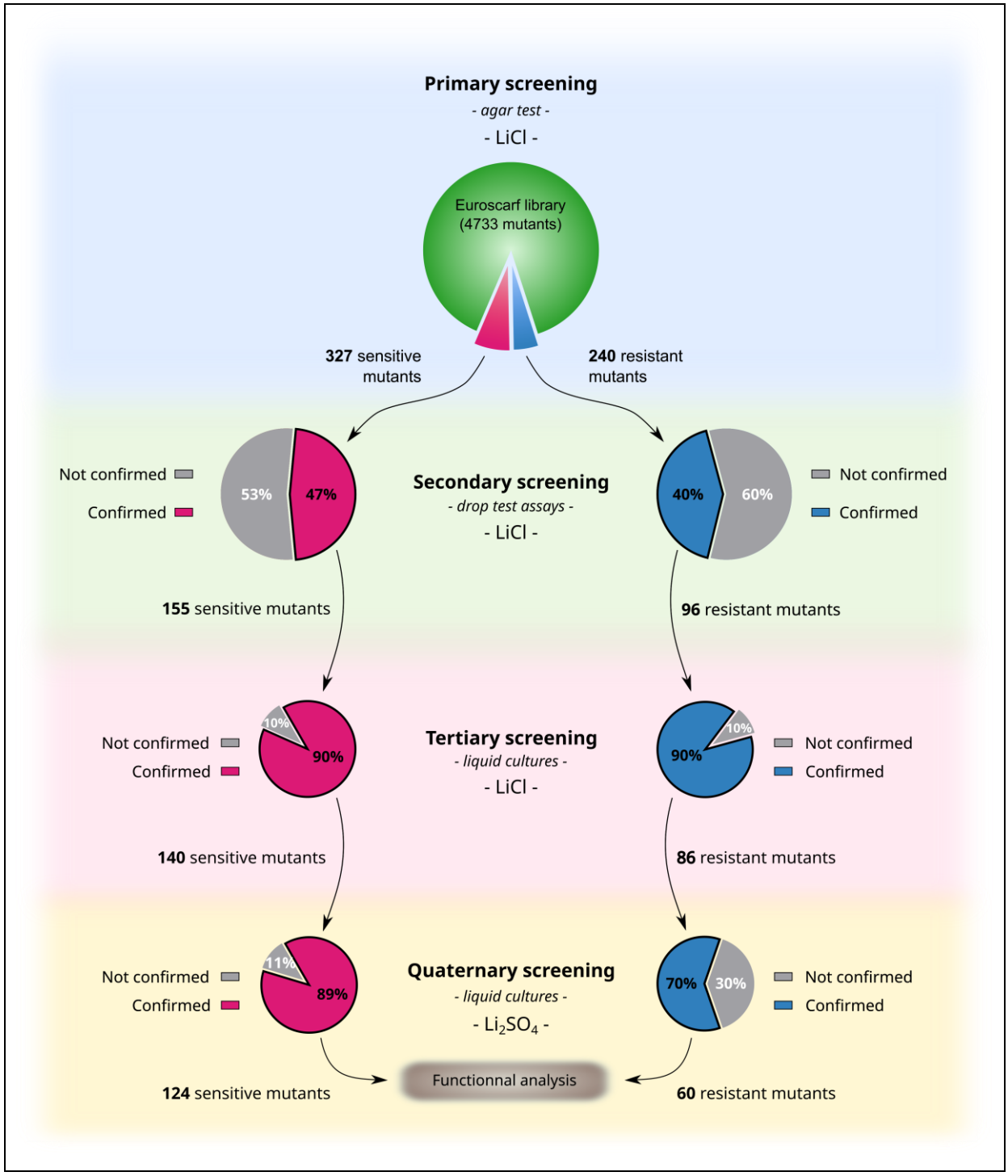

Figure 1: Overview of the different steps of the deletomics screening to identify the mutants sensitive and resistant to lithium. The number of selected mutants is indicated for each step of the screening. The percentage of false positives is also denoted within the pie charts. Representative data from the primary, secondary, tertiary and quaternary screenings are presented in Supplemental Figure S1.

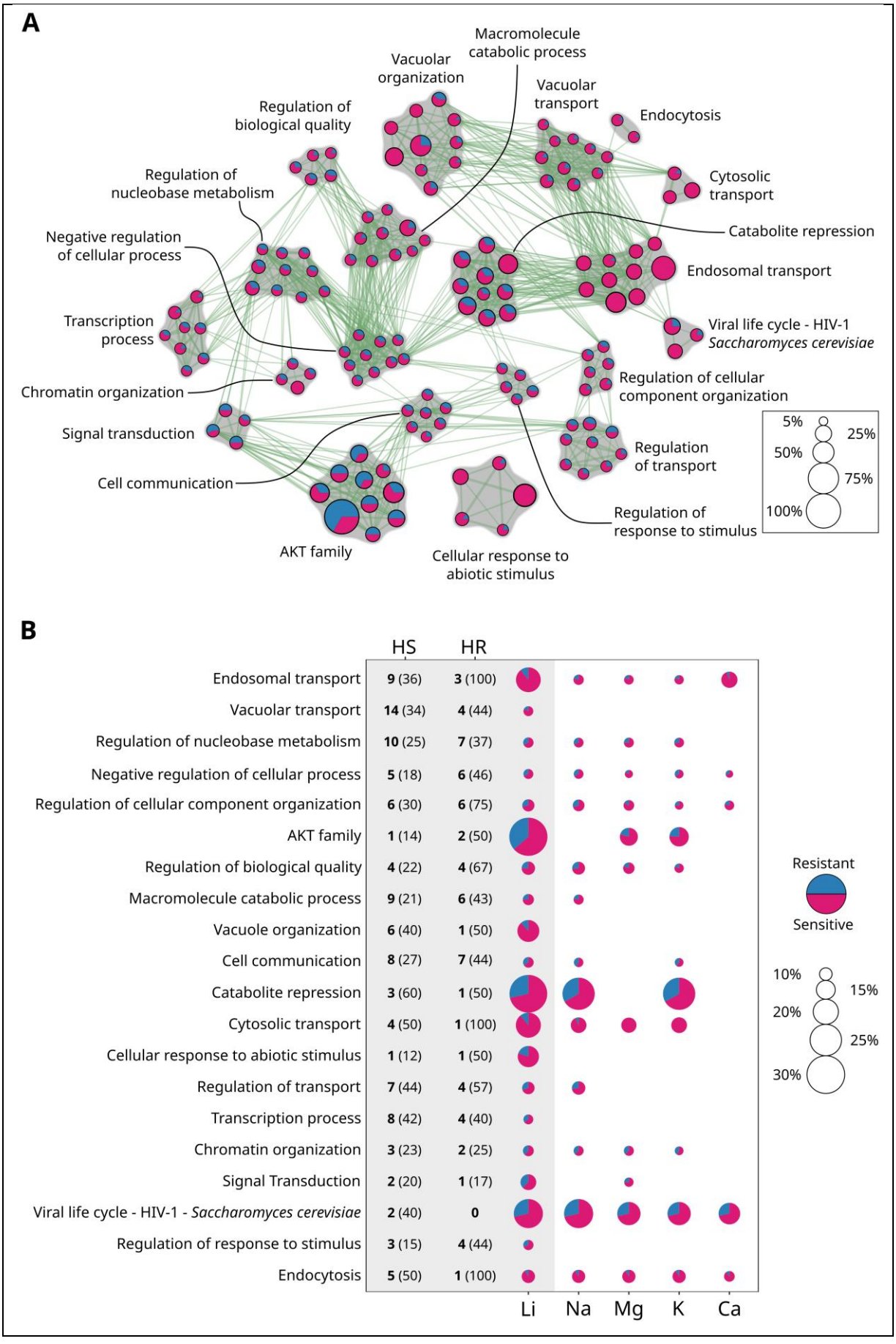
A
Macromolecule catabolic process
Vacuolar organization
Vacuolar transport
Endocytosis
Regulation of biological quality
Regulation of nucleobase metabolism
Cytosolic transport
Catabolite repression
Negative regulation of cellular process
Endosomal transport
Transcription process
Viral life cycle - HIV-1 Saccharomyces cerevisiae
Regulation of cellular component organization
Chromatin organization
Signal transduction
Regulation of transport
Cell communication
Regulation of response to stimulus
AKT family
Cellular response to abiotic stimulus
5%
25%
50%
75%
100%
B
HS
HR
Endosomal transport 9 (36) 3 (100)
Vacuolar transport 14 (34) 4 (44)
Regulation of nucleobase metabolism 10 (25) 7 (37)
Negative regulation of cellular process 5 (18) 6 (46)
Regulation of cellular component organization 6 (30) 6 (75)
AKT family 1 (14) 2 (50)
Regulation of biological quality 4 (22) 4 (67)
Macromolecule catabolic process 9 (21) 6 (43)
Vacuole organization 6 (40) 1 (50)
Cell communication 8 (27) 7 (44)
Catabolite repression 3 (60) 1 (50)
Cytosolic transport 4 (50) 1 (100)
Cellular response to abiotic stimulus 1 (12) 1 (50)
Regulation of transport 7 (44) 4 (57)
Transcription process 8 (42) 4 (40)
Chromatin organization 3 (23) 2 (25)
Signal Transduction 2 (20) 1 (17)
Viral life cycle - HIV-1 - Saccharomyces cerevisiae 2 (40) 0
Regulation of response to stimulus 3 (15) 4 (44)
Endocytosis 5 (50) 1 (100)
Li
Na
Mg
K
Ca
Resistant
Sensitive
10%
15%
20%
25%
30%

752

Figure 2: Functional enrichment analyses of resistant and sensitive mutants to lithium (A) or to alkali and alkaline-earth metals (B). The proportion of genes involved in the resistance (blue) and sensitivity (magenta) phenotypes is represented by pie charts inside each node (function) (A) or each functional cluster (B). (A) The size of each node/functional cluster corresponds to the number of genes found in a given category divided by the total number of genes in this category and expressed as a percentage. Green lines represent gene overlaps between two functions, and the edge width is proportional to the number of shared genes. (B) The number of Li high-sensitivity (HS) and high-resistance (HR) mutants are displayed on the left. Values in brackets denote the percentage of HS and HR mutants among the total number of mutants found in the functional analysis. The enrichment maps were built using Metascape and visualized with either Cytoscape (A) or the Scatterpie package in R (B).

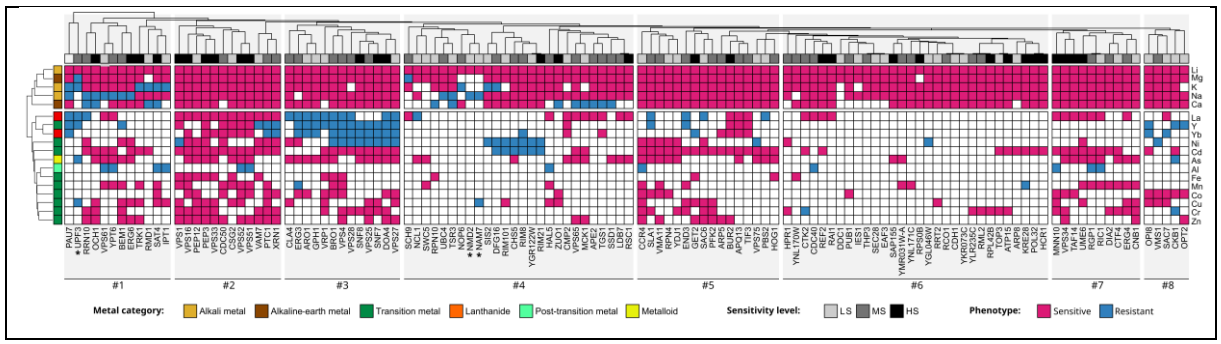

Figure 3: Cross-comparison of lithium-sensitive mutants versus other metals. The y-axis corresponds to metallic stressors. The x-axis represents a hierarchical clustering of the genes deleted that confer a sensitive phenotype to Li. Mutants exhibiting a sensitivity or resistance phenotype are shown in magenta and blue, respectively. Clusters 1 to 8 include mutants with a similar profile of sensitivity or resistance to metals. Asterisks indicate the three mutants that are specifically sensitive to Li. LS: low sensitivity; MS: medium sensitivity; HS: high sensitivity.

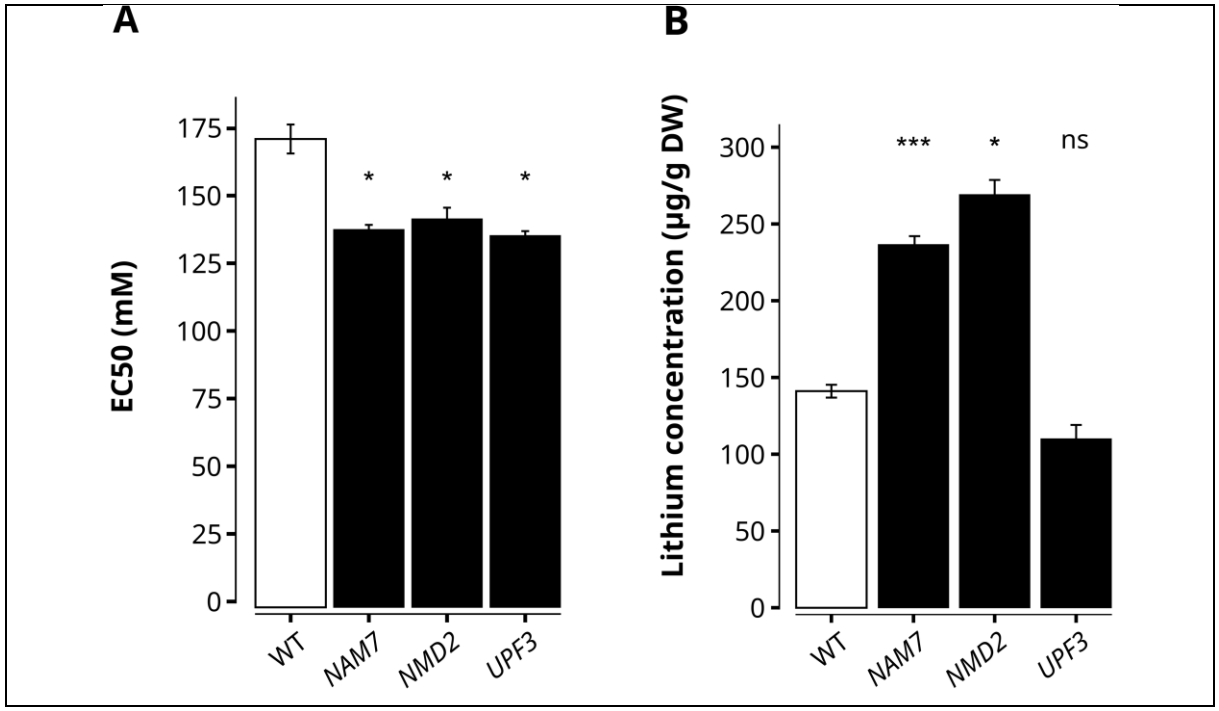

Figure 4: Sensitivity level and lithium accumulation by lithium-specific sensitive mutants. (A) EC50 values for LiCl for the three mutants and the WT. Data are the means (+/- SE) of three independent liquid cultures. A *t* test comparison between the mutants and the WT was carried out. (B) Yeast Li concentrations after one hour of exposure to 100 mM LiCl. Data are the means of five and three independent cultures for the WT and the mutants, respectively. Two-tailed Student's *t tests* to compare the different mutants to WT were performed. For all experiments: *<0.05; ***<0.001; ns: not significant.

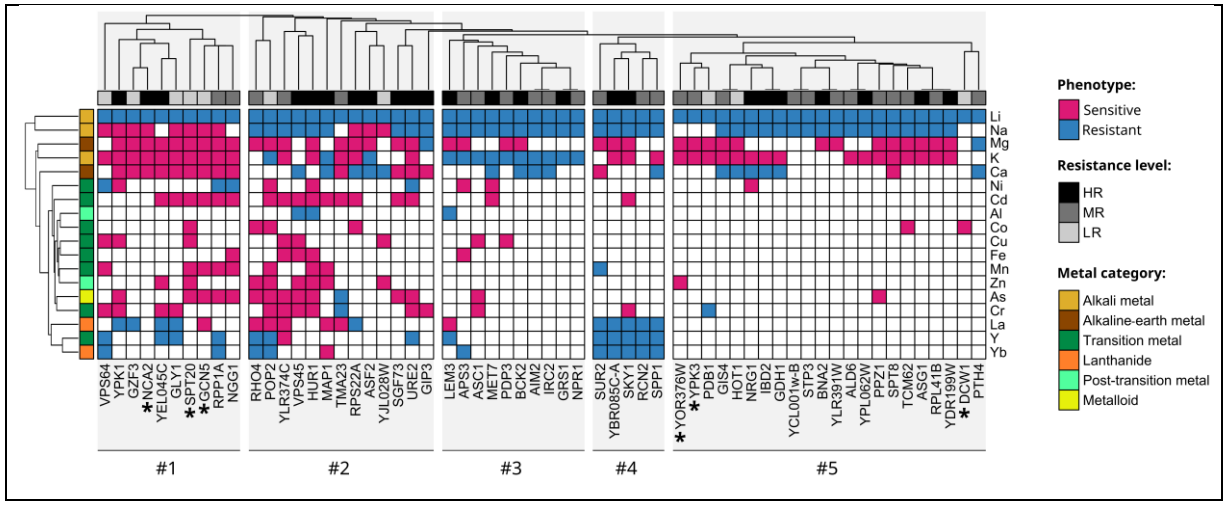

Figure 5: Cross-comparison of lithium-resistant mutants versus other metals. The y-axis corresponds to metallic stressors. The x-axis represents a hierarchical clustering of the genes deleted that confer a resistance phenotype to Li. Mutants exhibiting a sensitivity or resistance phenotype are shown in magenta and blue, respectively. Clusters 1 to 5 gather mutants with a similar profile of sensitivity or resistance to metals. Asterisks denote the six mutants that are specifically resistant to Li. LR: low resistance; MR: medium resistance; HR: high resistance.

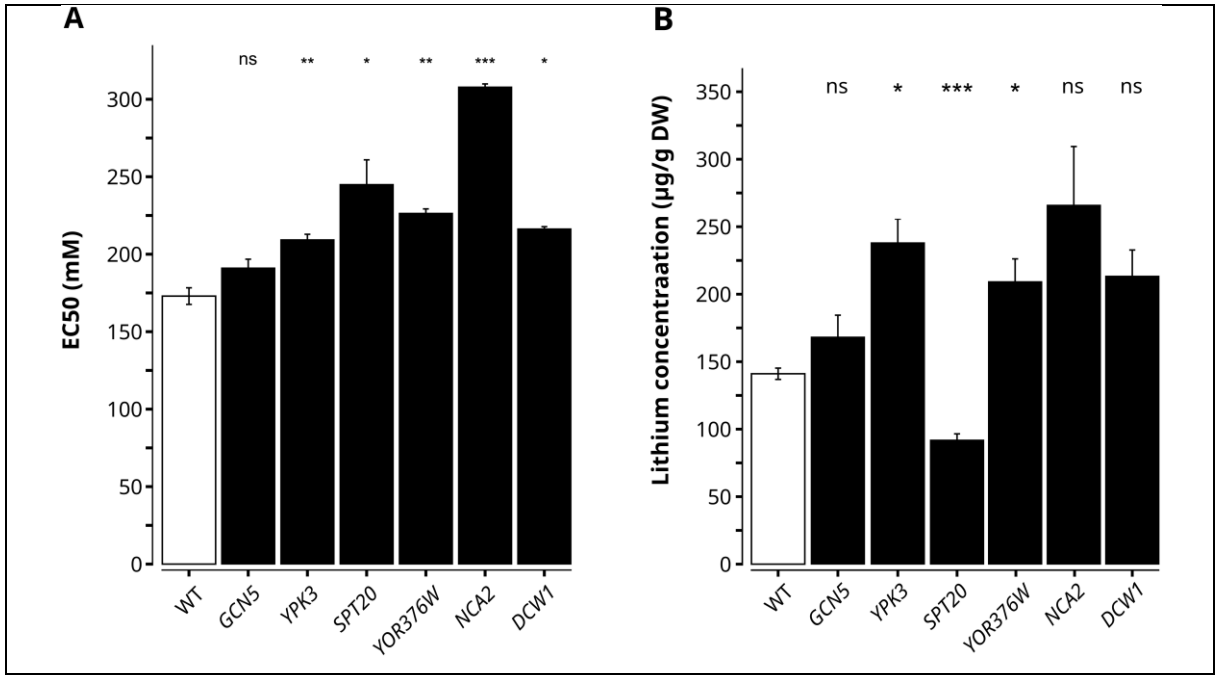

Figure 6: Resistance level and lithium accumulation by lithium-specific resistant mutants. (A) EC50 values for LiCl for the six mutants and the WT. Data are the means (+/- SE) of three independent liquid cultures. A *t* test comparison between the mutants and the WT was carried out. (B) Yeast Li concentrations after one hour of exposure to 100 mM LiCl. Data are the means of five and three independent cultures for the WT and the mutants, respectively. Two-tailed Student's *t tests* to compare the different mutants to WT were performed. For all experiments: *<0.05; **<0.01; ***<0.001; ns: not significant.

Supplemental data

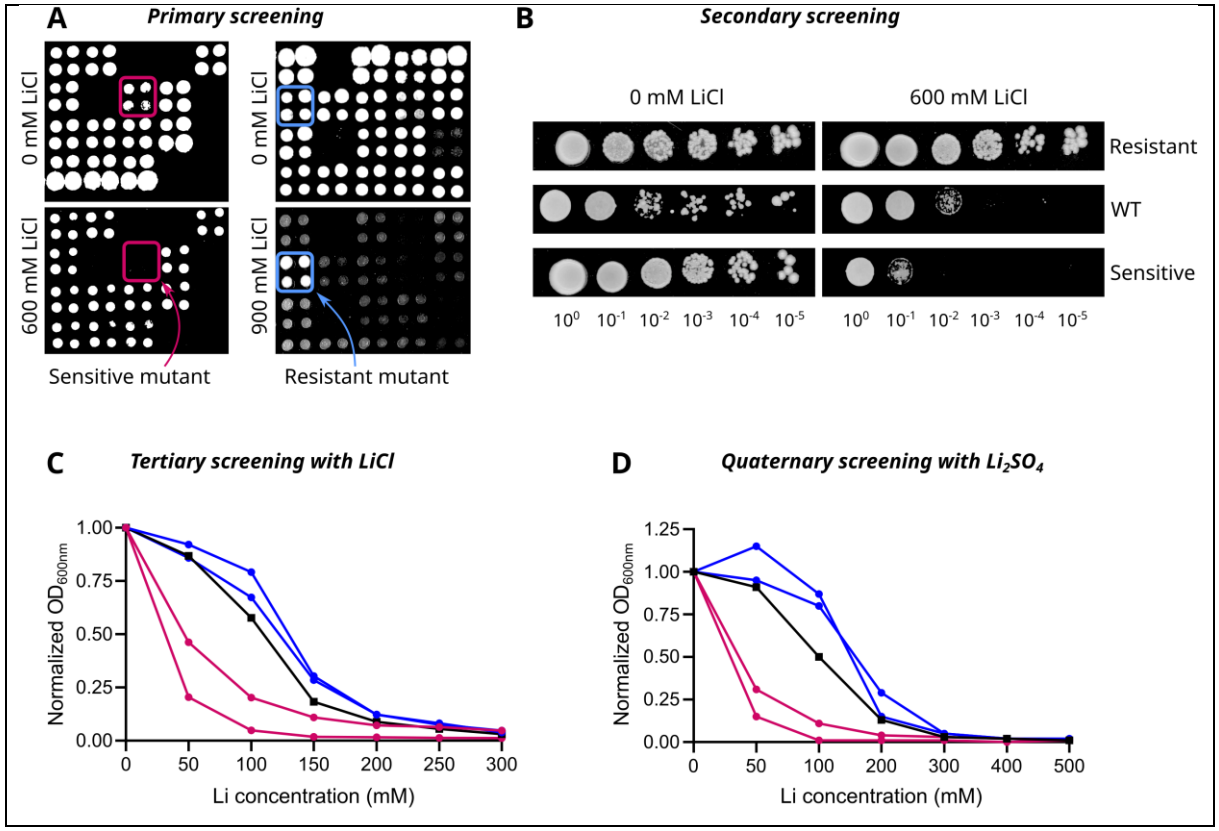

Supplemental Fig. S1: Representative data from the four screens of the Euroscarf deletion mutant library in the presence of Li. (A) Representative growth test of the primary screening. Four replicas per mutant were performed on the same plate. Putative Li-sensitive (magenta) and Li-resistant (blue) mutants are highlighted. (B) Drop test confirmation of the sensitive and resistant phenotypes by a secondary screening. Tenfold serial dilutions of yeast saturation cultures were deposited on the medium. The mutants were considered sensitive when they exhibited less colony-forming ability than WT. Conversely, the mutants were considered resistant when they exhibited better colony-forming ability than WT. (C) LiCl concentration-dependent growth of the mutants (tertiary screening). (D) Li concentration-dependent growth of the mutants under Li_2SO_4 (quaternary screening). The OD data were normalized to those obtained in Li-free medium, and a growth percentage in relation to the WT was calculated. (C-D) Blue: resistant mutant; magenta: sensitive mutant; black: WT.

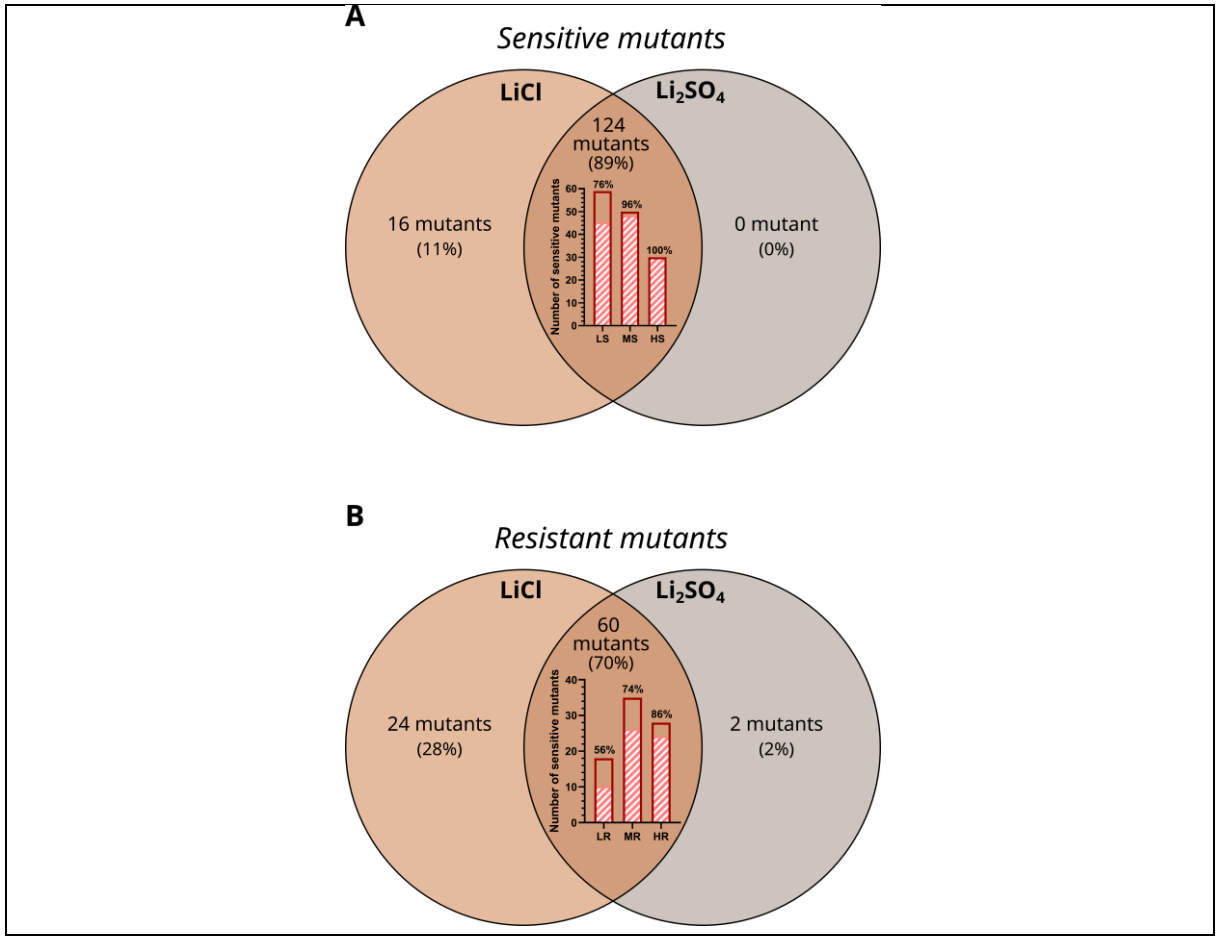

Supplemental Fig. S2: Venn diagram presenting the number of mutants sensitive (A) or resistant (B) to LiCl (red) and Li_2SO_4 (grey). The distribution of mutants in each category is denoted in parentheses. The numbers of low-sensitivity (LS), medium-sensitivity (MS), high-sensitivity (HS), low-resistance (LR), medium-resistance (MR) and high-resistance (HR) mutants are shown by hatching within the bars. The red bars represent the total number of mutants in each category identified in the tertiary screening with LiCl. The proportion of mutants in each category that were conserved after quaternary screening with Li_2SO_4 is displayed above the bars.

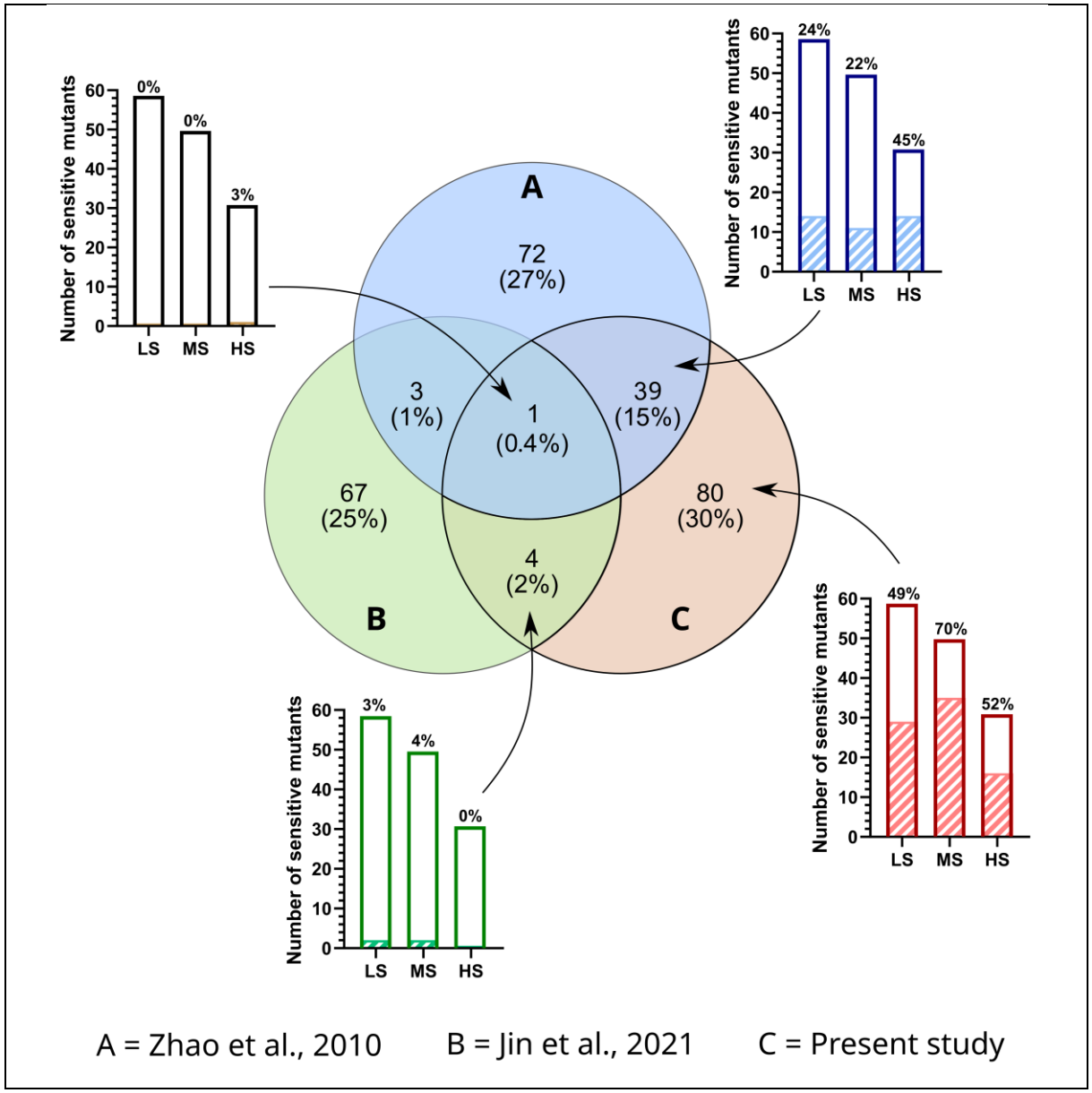

Supplemental Fig. S3: Venn diagram comparing the number of lithium-sensitive mutants identified from three lithium screening studies of yeast deletion mutant libraries. (A) Jin et al., (2021) in the presence of $LiPF_6$, (B) Zhao et al., (2010) in the presence of LiCl and (C) our study after quaternary screening in the presence of LiCl and Li_2SO_4. The percentage distribution of mutants in each category is denoted in parentheses.

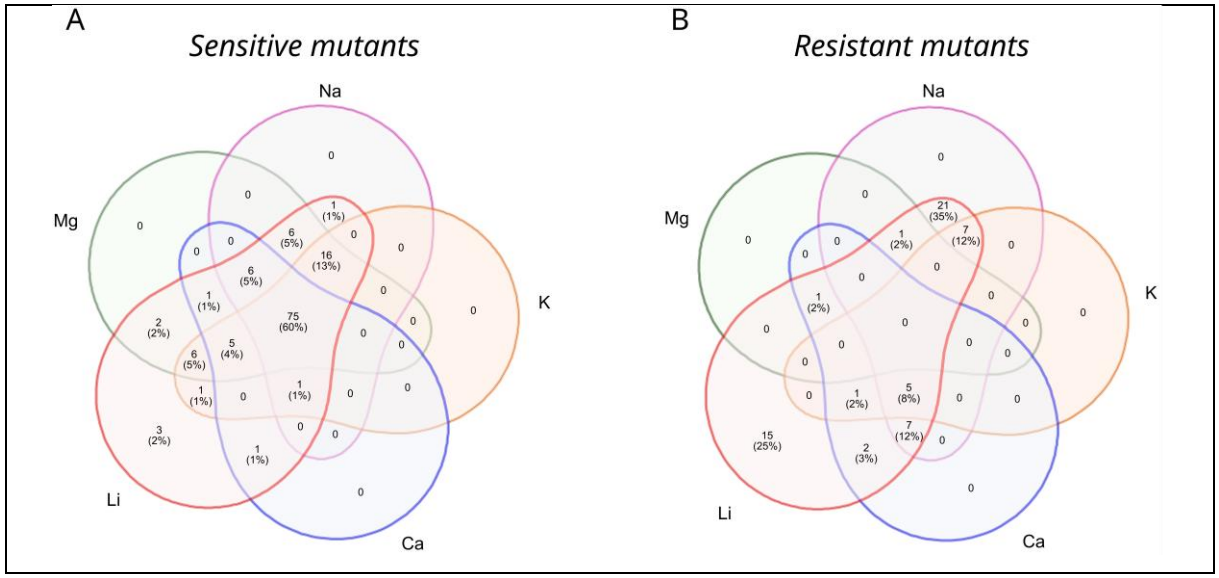

Supplemental Fig. S4: Venn diagram presenting the number of mutants sensitive (A) or resistant (B) to lithium and alkali metals or alkaline earth metals. The percentage distribution of mutants in each category is given in parentheses.